E·MRS Strasbourg (France)

ELSEVIER

MANUSCRIPT COVER PAGE FORM

E-MRS Symposium : G – Functional Materials for Micro and Nano Systems
Paper Number : G 06 01
Title of Paper : Ab initio study of NO_x compounds absorption on SnO_2 surface

Corresponding Author : J. Daniel Prades García

Full Mailing Address : Facultat de Física – Departament d'Electrònica
Martí i Franquès,1
08028 – Barcelona
SPAIN

Telephone : +34 93 40 39 147
Fax : + 34 93 40 21 148
E-mail: dprades@el.ub.es

Ab initio study of NO_x compounds <mark>adsorption</mark> on SnO_2 surface

J.D. Prades[1], A. Cirera[1], J.R. Morante[1], J.M. Pruneda[2,3], P.Ordejón[2]

[1] EME/CeRMAE/IN[2]UB, Dept. d'Electrònica, Universitat de Barcelona, C/. Martí i Franquès, 1, E-08028

Barcelona, Spain

[2] Institut de Ciències de Materials de Barcelona (ICMAB), CSIC, Campus de la UAB, E-08193,

Cerdanyola del Vallès, Spain

[3] Department of Physics, University of California at Berkeley, Berkeley, California 94720, USA

Abstract:

An ab initio study of the adsorption processes on NO_x compounds on (110) SnO_2 surface is presented with the aim of providing theoretical hints for the development of improved NO_x gas sensors. From first principles calculations (DFT-GGA approximation), the most relevant NO and NO_2 adsorption processes are analyzed by means of the estimation of their adsorption energies. The resulting values and the developed model are also corroborated with experimental desorption temperatures for NO and NO_2, allowing us to explain the temperature-programmed desorption experiments. The interference of the SO_2 poisoning agent on the studied processes is discussed and the blocking adsorption site consequences on sensing response are analyzed.

Key words:

AB INITIO, SnO_2, GAS SENSOR, NO, NO_2, SO_2, POISONING

1.- Introduction:

Developing new solid state gas sensors with improved properties carries with it an obvious close relationship between the sensing performance of the active materials and their surface chemical activity. The theoretical study of such surface-absorbate interactions provides a valuable tool to get superior performances that are unattainable using only a trial-and-error approach together with a powerful analytic methodology to explain the experimental data.

Tin dioxide (SnO_2) plays a key role as one of the more representative sensing materials in solid state gas sensors [1], presenting a significant surface reactivity with many important reducing (CO, NO) and oxidizing gases (O_2, NO_2) [2,3]. The present article deals with sensing mechanisms and processes concerning the detection of NO_x using SnO_2. Detection of NO_x is clearly important because it is a well-known environmental pollutant with harmful consequences for human health [4]. However, to explain the sensing behavior it is necessary to keep in mind that there exist interfering processes poisoning the surface [5] and that these can dramatically change the effective adsorptions of the target species and, therefore, their eventual detection. In the case of the SnO_2 surface, SO_2 is one of the more relevant poison specimens [6]. Thus, in the present analysis, its effects have also been studied in order to point up the consequences of the poisoning process on the sensing mechanisms.

Nowadays, first-principles methodologies based on density functional theory (DFT) can provide precise calculations of the energetic and vibrational properties of the adsorption [7]. Moreover, faster codes and new computational facilities allow dealing with numbers of surface-absorbate configurations in moderate computing times.

In this context, the aim of the present work is to provide theoretical hints for the development of improved NO_x gas sensors using SnO_2 as the base sensing material. The surface orientation relevance is discussed, and the most significant adsorption sites of NO_x are identified. Regarding SO_2 as poisoning specimen, its adsorption sites are located and the dependence of the poisoning effect with technologically accessible parameters is discussed.

2.- Calculation Details:

The first-principles methodology we used is based on density functional theory [8,9] (DFT) as implemented in the SIESTA code [10,11]. We made use of the generalized gradient approximation (GGA) for the exchange-correlation functional [12] and norm-conserving Troullier-Martins pseudopotentials [13] in Kleinman-Bylander factorization form [14]. The solutions of the Kohn-Sham equations are expanded as a linear combination of atomic pseudo-wave-functions of finite range. For all atomic species double ζ plus polarization orbitals basis-sets were used. Total energy convergence is guaranteed below 10meV, as is usual in this kind of calculations [15]. A real space mesh cut-off of 250Ry and a reciprocal space grid cut-off of approximately 15Å were used. The structural relaxations were done by means of a conjugate gradient minimization of the energy, until the forces on all the atoms were smaller than 0.04eV/Å (which provides relaxed total energy values more stable than 10meV). No constraints were imposed in the relaxation where forces were calculated as analytical derivatives of the total energy [16]. Spin polarization was also considered in the total energy computations, and basis set superposition error [17] (BSSE) was corrected in the calculated adsorption energies.

3.- Results and discussion:

3.1- Surface modeling:

It is commonly accepted that the facets of a crystal are those that minimize the total surface energy E_{surf} [18]. Consequently, for a given material, the most common (and relevant) faceting orientation will have the lowest E_{surf}. Therefore, we calculated the surface energies of several low index facets of SnO_2-cassiterite —also known as rutile or tetragonal phase, space group $P4_2mnm$, lattice parameters $a = b = 4.74$Å $c = 3.19$Å and two nonsymmetry-equivalent atoms at $(0.0,0.0,0.0)_{Sn}$ and $(0.305,0.305,0.0)_O$ [2]— were calculated in order to select the surface on which the adsorption processes would be analyzed. The initially considered low-index orientations are (110), (100), (101) and (001), which are accepted as some of the most common SnO_2-cassiterite faceting surfaces [19].

E_{surf} values were calculated following the procedure and definitions described in [19,20], and the results compared with values from the literature, are shown in Table 1. Our calculated data are in acceptable agreement with the literature and provide confidence in the accuracy of the calculation framework used. TiO_2 results are shown for comparison with another cassiterite system where (110) is also the lowest surface energy [21]. Therefore, in the following sections, adsorption phenomena will be studied over this surface orientation.

3.2.- Adsorption energy modeling:

To be able to estimate the energy change involved in the process of adsorption of a molecule onto a clean surface, we built models of 1) the clean surface slab, 2) the molecule, and 3) the surface plus the molecule system. For all three of these models, total energy calculations were performed, allowing us to evaluate the total energy balance of the adsorption process (so called adsorption energy E_{abs}) as follows:

$$E_{Tinitial} = E_{T(clean\ surface)} + E_{T(molecule)}$$

$$E_{Tfinal} = E_{T(clean\ surface+molecule)}$$

$$E_{abs} = \Delta E_T = E_{Tfinal} - E_{Tinitial} \tag{1}$$

Accordingly, a negative value of E_{abs} means that the adsorption is energetically favorable, it being possible for this to occur spontaneously without entropic considerations (DFT deals with the ground state at 0K).

It is necessary to ensure the effective cancellation of errors between the large energies that appear in equation (1). For this, adequate conditions were considered [7]. It has been verified that, in our case, a 2 layer thick slab is enough to ensure the stability of the adsorption energy values. Additionally, to ensure that the absorbed compound will not interact with periodic images of the slab, a 12Å vacuum thickness and a 2x1 unit cell slab width were used.

Moreover, the adsorption analysis requires several complementary steps: location of possible surface adsorption sites, also considering vacant sites, molecular modeling and, finally, adsorption modeling of NO_x and SO_2 compounds.

Figure 1 shows the slab model used for the adsorption on the SnO_2-cassiterite(110) surface. In order to obtain realistic values, surface relaxation was necessary (Figure 1 also presents the relaxed slab). Surface relaxation shows how six-fold coordinated Sn atoms (Sn_{6c}) tend to move outside the surface plane whereas five-fold coordinated Sn atoms (Sn_{5c}) tend to move inside. A similar behavior on (110) surface relaxation has been observed by other authors [22].

Two relevant adsorption sites appear to be a natural choice for the stoichiometric surface: a bridging site around bridging-oxygen [O_{Bridg}] and an inplane site around Sn_{5c} and the neighboring O_{3c} [$Sn_{InPlane}$]. In addition, O_{Bridg} appears at first glance, to be the most clear vacancy formation site [$O_{BridgVac}$] [15]. Consequently, two additional adsorption sites will be considered: a single O_{Bridg} vacancy (or a 50% reduced surface as long as there are only 2 nonequivalent O_{Bridg} atoms per slab) and a double O_{Bridg} vacancy site (or a 100% reduced surface). Finally, the adsorption of a molecule between an inplane Sn_{5c} and an O_{Bridg} vacancy [$O_{BridgVac}$-$Sn_{InPlane}$] was considered for NO_2 and SO_2.

As long as a good description of the absorbed molecules is necessary to obtain credible theoretical predictions, Table 2 presents the molecular models used and the obtained energetic and geometric parameters compared with those in the literature. It is worth noting that the agreement achieved is comparable with the commonly accepted discrepancy described in the literature [24].

Table 3 summarizes the calculated E_{abs} of NO and NO_2 on the considered adsorption sites. Adsorption temperature results are obtained by means of the well known Redheat equation, which links the $|E_{abs}|$ of a process with its maximum desorption rate temperature (T_{MDR}) in a temperature-programmed desorption (TPD) experiment [30]. Adjusting parameters were set according to the experimental conditions of [31] where an experimental TPD spectrum can be found for NO and NO_2 desorption from $SnO_2(110)$ surface (Figure 2).

We recall that our model only provides energies (and their corresponding desorption temperatures) for the concrete adsorption configurations analyzed. In contrast, an experimental TPD spectrum provides the temperature range at which a given species is desorbed by considering a plethora of adsorption configurations present in the real sample. Consequently, we would expect the calculated temperatures to

belong to the corresponding experimental TPD signal range. It is remarkable, therefore, how theoretical predictions of T_{MDR} for the few adsorption cases considered fall within the wide experimental desorption peaks from [31].

Our results suggest that O_{Bridg} sites are the most energetically favorable for NO. This behavior is compatible with the observed fact that NO reduces the SnO_2, given that NO is expected to bond with a surface oxygen to be able eventually to remove it reducing the surface [1]. Instead, however, $O_{BridgVac}$ are involved in the energetically preferred adsorption sites for NO_2.

For these preferred adsorption sites, a dependency of the adsorption energy with the reduction state of the surface is observed. In both cases (NO and NO_2) surface reduction seems to diminish slightly the adsorption energy on O_{Bridg} and $O_{BridgVac}$ sites respectively.

It is important to note that the difference in the preferred adsorption sites between NO and NO_2 suggests that by generating vacant sites and adjusting their density, the adsorption feasibility of NO versus NO_2 on an eventual SnO_2-based gas sensor may be changed. This leads to a technological suggestion in the preparation of the sensing material.

Concerning the SO_2 adsorption, Table 4 summarizes the calculated E_{abs} of SO_2 on several sites. As for NO_2, the preferred adsorption sites also involve $O_{BridgVac}$ but, in this case, it seems that the more reduced the surface is, the stronger is the SO_2 adsorption that takes place. This different behavior with respect to the surface reduction percentage has dramatic consequences on the interference of SO_2 when trying to detect NO_2.

It is a known fact that SO_2 avidly saturates NO_2 adsorption sites, reducing the SnO_2 sensing capability [6]. In order to shed some light on this, Figure 3 shows the E_{abs} values of the most energetically favorable adsorptions of NO_2 and SO_2 as a function of the surface reduction. At every reduction percentage, the same adsorption configuration is considered for both compounds, so a competitive situation is analyzed. It is confirmed that the strongest adsorption within the studied cases corresponds to SO_2, which is a theoretical behavior compatible with the experimental evidence of the poisoning effect.

6

It is also clear that SO_2 absorbs stronger than NO_2 in stoichiometric and also in 100% reduced configurations. However, for intermediate surface reductions, NO_2 seems to be absorbed stronger than SO_2. This suggests that the poisoning strength is dependant on the surface reduction state and may even be reduced for intermediate bridging-oxygen vacancy densities on the $SnO_2(110)$ surface. This again points out a technological hint for the preparation of the sensing material.

Regarding NO, it has been shown that its preferred adsorption sites are O_{Bridg}. Therefore, it may seem that there is no competitive behavior with SO_2. However, Table 3 shows how, for intermediate reductions, the adsorption of NO on O_{Bridg} under the presence of an SO_2 occupying an $O_{BridgVac}$ site (Table 3 case #) is slightly stronger than in the noninteracting (case c). These results suggest that in spite of the fact that the preferred adsorption sites for NO and SO_2 are different, a cross-influence may occur between both compounds, and this would merit further analysis.

4.- Conclusions:

A theoretical approach to the NO and NO_2 adsorption on $SnO_2(110)$ based on ab initio calculations has been presented. Bridging-oxygen sites and bridging-oxygen vacancy sites were identified as the most relevant adsorption sites for NO and NO_2 respectively. This difference may suggest that adjusting oxygen vacant sites density the adsorption feasibility of NO versus NO_2 on an eventual SnO_2-based gas sensor may be changed.

Regarding the poisoning by SO_2, bridging-oxygen vacancies seem to be the most favorable adsorption sites, suggesting a competitive behavior with NO_2. Theoretical trends indicate that NO_2 adsorption strength decreases with the surface reduction while for SO_2, it increases. Such a different evolution insinuates that the poisoning effect may be diminished by means of adjusting the SnO_2 surface reduction to intermediate values. In the case of NO, no competitive behavior with SO_2 is expected because of their preferred adsorption sites being different, but further study may be necessary to analyze an eventual cross-influence.

To conclude, under the light of the presented adsorption sites and their corresponding maximum desorption rate temperatures, one can see that adjusting the working conditions (i.e, working temperature)

of an eventual SnO_2-based gas sensor will determine the reversibility of the adsorption at a given site. Working at temperatures around 300ºC, where the low desorption rate may ease the fast saturation of the adsorption sites, thus spoiling the sensing properties, seems to be particularly problematic. In any case, to make theoretical predictions on the optimum working conditions of a real sensor, a more complex model is necessary, for example, one including the cross-influence of OH groups due to humidity.

Acknowledgements:

References:

[1] W. Göpel and K.D.Schierbaum, SnO$_2$ sensors: current status and future prospects, Sensors and Actuators B, Chemical, 26-27 (1995) 1-12.

[2] M. Batzill and U. Diebold, The surface and materials science of tin oxide, Progress in Surface Science., 79 (2005) 47-154.

[3] G. Sverveglieri, Recent developments in semiconducting thin-film gas sensors, Sensors and Actuators B, Chemical, 23 (1995) 103-109.

[4] A. Fritz and V. Pitchon, The current state of research on automotive lean NO$_x$ catalysis, Applied Catalysis B-Environmental, 13 (1997) 1-27.

[5] D.E. Williams , G.S. Henshaw and K.F.E. Pratt, Detection of sensor poisoning using self-diagnostic gas sensors, J. Chem. Society - Faraday Transactions, 91 (1995) 3307-3308.

[6] B. Ruhland, T. Becker, G. Muller, Gas-kinetic interactions of nitrous oxides with SnO$_2$ surfaces, Sensors and Actuators B, Chemical, 50 (1998) 85-94.

[7] K.M. Neyman and F. Illas, Theoretical aspects of heterogeneous catalysis: Applications of density functional methods, Catalysis Today, 105 (2005) 2-16.

[8] P. Hohenberg and W. Kohn, Inhomogeneous electron gas, Phys. Rev., 136 (1964) B864-B871.

[9] W. Kohn and L.J. Sham, Self-consistent equations including exchange and correlation effects, Phys. Rev., 140 (1965) A1133-A1138.

[10] P. Ordejón, E. Artacho, and J.M. Soler, Self-consistent order-N density-functional calculations for very large systems, Phys. Rev. B, 53 (1996) R10441-R10444.

[11] J.M. Soler, E. Artacho, J.D. Gale, A. García, J. Junquera, P. Ordejón and D. Sánchez-Portal, The SIESTA method for ab initio order-N materials simulation, J. Phys: Condens Matter, 14 (2002) 2745-2779.

[12] J. P. Perdew, K. Burke and M. Ernzerhof, Generalized Gradient Approximation made simple, Phys. Rev. Lett., 77 (1996) 3865-3868.

[13] N. Troullier and J. L. Martins, Efficient pseudopotentials for plane-wave calculations, Phys. Rev. B, 43 (1991) 1993-2006.

[14] L. Kleinman and D.M. Bylander, Efficacious form for model pseudopotentials, Phys. Rev. Lett., 48 (1982) 1425-1428.

[15] J. Oviedo and M.J.Gillan, First-principles study of the interaction of oxygen with the SnO2(110) surface, Surf. Sci., 490 (2001) 221-236.

[16] D. Sánchez-Portal, P. Ordejón, E. Artacho, J. M. Soler, Density-functional method for very large systems with LCAO basis sets, Int. J. Quantum Chem., 65 (1997) 453-461.

[17] S.F. Boys and F.F. Bernardi, Calculation of small molecular interactions by differences of separate total energies - Some procedures with reduced errors, Mol. Phys., 19 (1970) 553-566.

[18] A.S. Barnard and P. Zapol., Effects of particle morphology and surface hydrogenation on the phase stability of TiO$_2$, Phys. Rev. B, 70 (2004) 235403-235416.

[19] J.Oviedo and M.J.Gillan, Energetics and structure of stoichiometric SnO_2 surfaces studied by first-principles calculations, Surf. Sci., 463 (2000) 93-101.

[20] W. Zhu and P.Wu, Surface energetics of hydroxyapatite: a DFT study, Chem. Phys. Lett., 396 (2004) 38-42.

[21] M. Ramamoorthy, D. Vanderbilt and R..D. King-Smith, First-principles calculations of the energetics of stoichiometric TiO2 surfaces, Phys. Rev. B, 49 (1994) 16721-16727.

[22] T.T. Rantala, T.S. Rantala and V. Lantto, Electronic structure of SnO_2 (110) surface, Mat. Sci. Semiconductor Processing, 3 (2000) 103-107.

[23] F.R. Sensato, R. Custódio, M. Calatayud, A. Beltrán, J. Andrés, J.R. Sambrano and E. Longo, Periodic study on the structural and electronic properties of bulk, oxidized and reduced SnO_2(110) surfaces and the interaction with O_2, Surf. Sci., 511 (2002) 408-420.

[24] S. Kurth, J.P. Perdew and P. Blaha, Molecular and solid-state tests of density functional approximations: LSD, GGAs, and meta-GGAs, Int. J. Quantum Chem., 75 (1999) 889-909.

[25] H. Dong, Y.-H. Ding and C.-C. Sun, Mechanism of HCS + O_2 reaction: hydrogen- or oxygen-transfer?, Phys. Chem. Chem. Phys., 7 (2005) 3711-3715.

[26] H. Orita and N. Itoh, Adsorption of N_2 and N_2O on Ni(755) surface: ab initio periodic density functional study, Surf. Sci., 550 (2004) 166-176.

[27] Z.-G.Wei, X.-R. Huang, S.-W. Zhang, Y.-B. Sun, H.-J. Qian and C.-C. Sun, A theoretical study on the potential energy surface of the 3C2 + NO reaction, J. Phys. Chem. A, 108 (2004) 6771-6777.

[28] J.-X. Zhang, J.-Y. Liu, Z.-S. Li and C.-C. Sun, Theoretical study on reaction mechanism of the fluoromethylene radical with nitrogen dioxide, J. Comp. Chem., 25 (2004) 1888-1894.

[29] K. Sendt and B.S. Haynes, Role of the direct reaction H_2S + SO_2 in the homogeneous Claus reaction, J. Phys. Chem. A, 109 (2005) 8180-8186.

[30] M.C. Desjonquères and D. Spanjard, Concepts in Surface Physics, Springer, 2nd ed., 1996.

[31] E.Leblanc, L.Perier-Camby, G.Thomas, R.Gibert, M.Primet and P.Gelin., NOx adsorption onto dehydroxylated or hydroxylated tin dioxide surface. Application to SnO2-based sensors, Sensors and Actuators B, Chemical, 62 (2000) 67-72.

[32] V. P. Zhdanov and B. Kasemo, Simulation of oxygen desorption from Pt(111), Surf. Sci., 415 (1998), 403-410.

Biography:

J. Daniel Prades: graduated in Physics at the University of Barcelona in 2005. Now he is PhD student in Department of Electronics of the same university. His current research is focused on first-principles modeling of electronic and vibrational properties of nanostructured metal oxides.

Dr. Albert Cirera: graduated in Physics at the University of Barcelona in 1996. He received his PhD in 2000 from the University of Barcelona, developing new technologies and their characterization for tin oxide gas sensor devices. He is currently associate professor and works in the field of sensors and its simulation, as scientist and coordinator in several related industrial projects.

Prof. Dr. Joan R. Morante: was born in Mataró (Spain). At 1980 he received the Ph D degree in Physics from the University of Barcelona. Since 1986 he is full professor of Electronics and director of the Electronic Materials and Engineering, EME, group. He has been dean of the Physics Faculty and academic advisor of the Electronic Engineering degree. He was director of the Electronics Department in the University of Barcelona which is associated unity to the Centre Nacional de Microelectronics at Bellaterra (Barcelona). Actually, he is research head of the EME group and co-director of the CEMIC, center of the Microsystems Engineering and director of the CeRMAE, reference center of advanced materials for energy from Generalitat of Catalunya. His activity is devoted to the electronic materials and technology, physics and chemical sensors, actuators, and microsystems. He has especial interest in nanoscience and micro&nanotechnologies. He has collaborated in international R&D projects as BRITE, GROWTH (micromechanics, microengineering, gas sensors, nanomaterials...), ESPRIT, IST (advanced devices, sensors, actuators, Microsystems, electronic systems,...), JOULE,...EUREKA, IBEROEKA and industrial projects. He is co-author of more than 400 works in international specialised journal and member of international committees and editorial boards in the field of electronic materials and technology, sensors&actuators and microsystems, and electronic systems. He has been distinguished with the research prize Narciso Monturiol and the "senior research distinction" award from the Generalitat of Catalunya (Spain) .

Dr. J. Miguel Pruneda: Marie Curie Fellow between the Department of Physics at UC Berkeley and the ICMAB. Graduated in physics at Universidad de Oviedo in 1997, and got the PhD in 2002 (Oviedo). After 3 years as a research associate at the department of Earth Sciences in the University of Cambridge studying materials for nuclear waste immobilization, joined the group of P.Ordejón. Interest in materials for nanotechnology and spintronic.

Prof. Dr. Pablo Ordejón: is Research Professor at the ICMAB-CSIC, in Barcelona. He studied physics at the Universidad Autonoma de Madrid (Spain), where he obtained his PhD in science in 1987, and afterwards he did a three years postdoctoral stay at the University of Illinois at Urbana-Champaign (USA). His research has focused on the development and application of efficient methods for electronic structure calculations in large and complex systems, and techniques for large scale atomistic simulations based on first-principles methods. He is Regional Editor of the journal Physica Status Solidi and was recently elected as Fellow of the American Physical Society.

Tables:

Table 1: Surface energy results for the considered SnO_2-cassiterite faceting orientations. Several references form the literature are given. Computational uncertainty is also shown when possible.

Surface	E_{surf} [J/m^2]		
	This work SnO_2 GGA	SnO_2 GGA [19]	TiO_2 LDA [21]
	<±0.20	<±0.20	
(110)	*1.01*	1.04	0.89
(100)	*1.32*	1.14	1.12
(101)	*1.49*	1.33	1.39
(001)	*1.87*	1.72	1.65

Table 2: Energetic and geometric first principles modeled parameters of several molecules involved in the adsorptions considered in this work. Reference values are from the literature.

Compound	Bond energy [eV]		Bond length [Å]		Angle [º]	
	This work	Ref.[24]	This work	Ref.	This work	Ref.
O_2	5.90	6.23 (calc.) 5.23 (exp.)	1.24	1.18 – 1.21 [25]	–	–
N_2	9.47	10.55 (calc.) 9.47 (exp.)	1.12	1.09 – 1.11 [26]	–	–
NO	7.03	7.45 (calc.) 6.63 (exp.)	1.17	1.12 – 1.17 [27]	–	–
NO_2	5.54	–	1.23	1.20 [28]	132	133-134 [28]
SO_2	5.91	–	1.49	1.48 [29]	112	109 [29]

Table 3: Calculated adsorption energies E_{abs} for NO_x on several adsorption sites of the $SnO_2(110)$ surface and maximum desorption rate temperature T_{MDR} estimated for the experimental conditions of [31]. Some configurations are not energetically favorable ($E_{abs} > 0$). Energetically favorable processes are labeled using letters in parentheses to identify them in Figure 2. For NO, a configuration with presence of SO_2 (#) is considered for later discussion on poisoning. Notice that NO_2 adsorption on a 100% reduced slab can appear with two different configurations: bonding one single O atom of the molecule (single bonded) or bonding both (double bonded).

Absorbate	Surface state	Adsorption site		E_{abs} [eV]	T_{MDR} [°C]	
NO	Stoichiometric slab	O_{Bridg}		**−1.32**	188	(a)
	Stoichiometric slab	$Sn_{InPlane}$		**−0.24**	52	(b)
	50% reduced slab	O_{Bridg}		**−1.18**	167	(c)
	50% reduced slab	*O_{Bridg} + (SO_2 in $O_{BridgVac}$)*		***−1.28***	–	(#)
	50% reduced slab	$O_{BridgVac}$		**−0.42**	89	(d)
	100% reduced slab	$O_{BridgVac}$		**−0.98**	153	(e)
NO$_2$	Stoichiometric slab	O_{Bridg}		**+1.51**	–	
	Stoichiometric slab	$Sn_{InPlane}$		**−0.52**	94	(v)
	50% reduced slab	$O_{BridgVac}$	(single bonded)	**−2.31**	502	(w)
	50% reduced slab	$O_{BridgVac}$-$Sn_{InPlane}$		**+0.34**	–	
	100% reduced slab	$O_{BridgVac}$	(single bonded)	**−2.02**	424	(x)
			(double bonded)	**−1.95**	400	(y)
	100% reduced slab	$O_{BridgVac}$-$Sn_{InPlane}$		**−2.11**	454	(z)

Table 4: Calculated adsorption energies E_{abs} for SO_2 on several adsorption sites of the $SnO_2(110)$ surface and maximum desorption rate temperature T_{MDR} estimated for the experimental conditions of [31]. Notice that, in contrast with the NO_2 case, calculations show that SO_2 adsorption on a 100% reduced slab may only be spontaneous ($E_{abs} < 0$) in one single O bonding configuration. Some configurations are not energetically favorable ($E_{abs} > 0$).

Absorbate	Surface state	Adsorption site		E_{abs} [eV]	T_{MDR} [°C]
	stoichiometric slab	O_{Bridg}		**+1.72**	–
	stoichiometric slab	$Sn_{InPlane}$		**−0.86**	128
	50% reduced slab	$O_{BridgVac}$	(single bonded)	**−2.05**	435
SO_2	50% reduced slab	$O_{BridgVac}$-$Sn_{InPlane}$		**+1.12**	–
	100% reduced slab	$O_{BridgVac}$	(single bonded)	**+0.26**	–
			(doble bonded)	**−2.56**	606
	100% reduced slab	$O_{BridgVac}$-$Sn_{InPlane}$		**−2.97**	741

Figure Captions:

Figure 1: Slab model of the SnO$_2$-cassiterite (110) surface. Relaxed and unrelaxed geometries are shown. Adsorption sites are highlighted and relevant surface atoms are identified.

Figure 2: Top: Experimental TPD spectra of NO and NO$_2$ desorbing form a dehydroxylated SnO$_2$(110) surface (reprinted from [31], with permission from Elsevier). Bottom: Calculated TPD spectra for NO and NO$_2$ considering all the configurations detailed in Table 3. One TPD spectrum was simulated (by means of solving the rate expression for desorption kinetics [30,32]) for each adsorption configuration with the experimental parameters given in [31]. For every configuration the temperature corresponding to its maximum desorption rate is indicated with a labeled arrow –see labels and T$_{MDR}$ values in Table 3–. Total spectra were obtained as the summation of the normalized single configuration spectra.

Figure 3: Adsorption energies E$_{abs}$ of NO$_2$ and SO$_2$ as a function of the SnO$_2$(110) surface reduction. Only stronger adsorptions and identical configurations are considered at every reduction percentage so a competitive situation is analyzed. Details on adsorption configurations of every data point is given in Table 3 and Table 4. Dotted lines are plotted as visual aids.

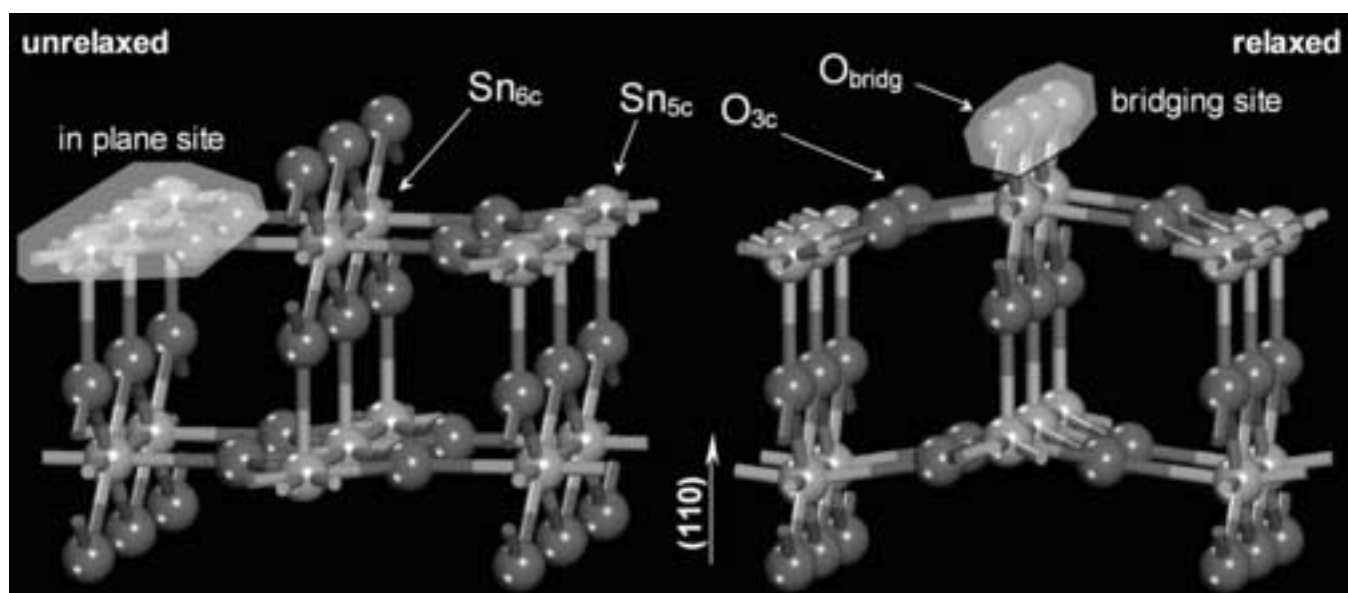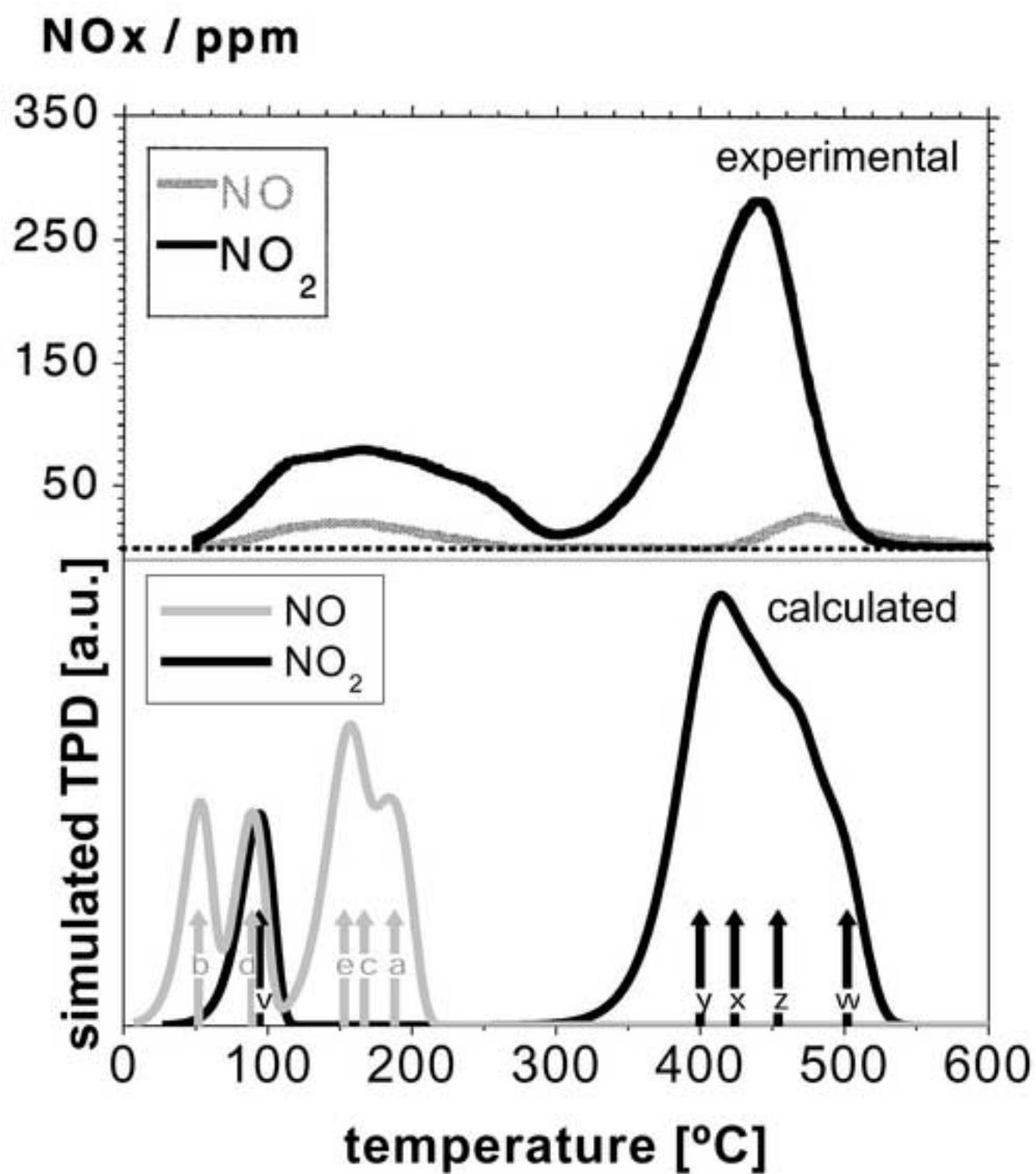**Figure 1**
Click here to download high resolution image